LETTERS

Arginine methylation at histone H3R2 controls deposition of H3K4 trimethylation

Antonis Kirmizis[1], Helena Santos-Rosa[1], Christopher J. Penkett[2], Michael A. Singer[3], Michiel Vermeulen[4], Matthias Mann[4], Jürg Bähler[2], Roland D. Green[3] & Tony Kouzarides[1]

Modifications on histones control important biological processes through their effects on chromatin structure[1–3]. Methylation at lysine 4 on histone H3 (H3K4) is found at the 5′ end of active genes and contributes to transcriptional activation by recruiting chromatin-remodelling enzymes[4,5]. An adjacent arginine residue (H3R2) is also known to be asymmetrically dimethylated (H3R2me2a) in mammalian cells[6], but its location within genes and its function in transcription are unknown. Here we show that H3R2 is also methylated in budding yeast (*Saccharomyces cerevisiae*), and by using an antibody specific for H3R2me2a in a chromatin immunoprecipitation-on-chip analysis we determine the distribution of this modification on the entire yeast genome. We find that H3R2me2a is enriched throughout all heterochromatic loci and inactive euchromatic genes and is present at the 3′ end of moderately transcribed genes. In all cases the pattern of H3R2 methylation is mutually exclusive with the trimethyl form of H3K4 (H3K4me3). We show that methylation at H3R2 abrogates the trimethylation of H3K4 by the Set1 methyltransferase. The specific effect on H3K4me3 results from the occlusion of Spp1, a Set1 methyltransferase subunit necessary for trimethylation. Thus, the inability of Spp1 to recognize H3 methylated at R2 prevents Set1 from trimethylating H3K4. These results provide the first mechanistic insight into the function of arginine methylation on chromatin.

Methylation at lysine and arginine residues within histones has been linked to gene expression[1–3]. Studies in mammalian cells have shown that arginine methylation of histones can influence both gene activation and repression. However, the precise mechanism employed by arginine methylation to exert its effects on the chromatin template is still unknown. In contrast, increasing evidence shows that lysine methylation modulates gene expression by recruiting downstream effector proteins. Recent findings showed that methylation at H3K4 (H3K4me) controls transcription activation by recruiting chromatin remodelling activities[4,5]. This recruitment can be specific for H3K4me3 (refs 7, 8), indicating that the three different methyl states of H3K4 (monomethylated, dimethylated and trimethylated) have distinct functions in gene expression. The Set1 complex is the enzyme that can mediate the methylation of H3K4, and various components of the complex regulate the establishment of the different methyl-H3K4 states[9–11].

To investigate the role of methylation at H3R2 in gene expression we raised an antibody against H3R2me2a. This modification is known to be catalysed by the mammalian CARM1/PRMT4 *in vitro*[12] and is affected by deletion of this methyltransferase in mouse embryonic fibroblasts[6]. Immunoblot analysis reveals that H3R2me2a is present *in vivo*, on mammalian and yeast histone H3 (Supplementary Fig. 1a, b). We confirmed the specificity of this antibody towards H3R2me2a by dot-blot analysis and peptide competition assays (Supplementary Fig. 1c, d). Most importantly, the antibody does not recognize histone H3 in yeast cells in which arginine 2 has been mutated to an alanine residue (H3R2A), a glutamine residue (H3R2Q) or a lysine residue (H3R2K) (Supplementary Figs 1e and 2).

To examine the specific function of H3R2 methylation, we used a high-resolution chromatin immunoprecipitation (ChIP)-on-chip analysis in yeast to determine its genome-wide distribution. We found that this mark is associated with both heterochromatin and euchromatin (Figs 1 and 2). Analysis of heterochromatin showed that H3R2me2a is present at all four heterochromatic regions in yeast: the two silent mating-type loci (*HMR* and *HML*), the ribosomal RNA-encoding DNA (*rDNA* repeat) and telomeres (Fig. 1a–d). In this analysis it became clear that all heterochromatic regions that were enriched in H3R2 methylation were also devoid of the active methyl mark H3K4me3 (Fig. 1a–d). Indeed, the decrease in H3R2me2a and increase in H3K4me3 levels can be used to define the boundaries of heterochromatic regions.

The presence of H3R2me2a at heterochromatic sites indicates that this methylation may be part of a signal to silence transcription. We therefore used yeast strains expressing the H3R2 mutants H3R2A and H3R2Q to test the role of this residue in heterochromatic silencing. We found that mutation of arginine 2 resulted in a severe loss of silencing in the *HMR*, telomere and *rDNA* loci, and to a moderate extent at the *HML* locus (Fig. 1e and Supplementary Fig. 3, left panels). These results indicate that arginine 2 on H3 is necessary for heterochromatic silencing, indicating a possible role for H3R2 methylation in this process.

We next considered the mechanism by which H3R2me2a may function to regulate heterochromatin. Comparison of the occupancy of key heterochromatic factors, such as Rap1p and Sir2p, with H3R2me2a enrichment indicates a coincidence at telomeric sites (compare Fig. 1d with Fig. 1f). However, when ChIP analysis of Rap1p and Sir2p was compared in wild-type (WT) and H3R2A strains the amount of binding of these two proteins at the heterochromatic sites was not changed (Fig. 1f). These results indicate that methylation at H3R2 functions at heterochromatin through a previously unobserved mechanism, which is independent of Rap1p and Sir2p recruitment. However, we cannot exclude the possibility that disruption of H3K4 methylation may contribute to the H3R2A phenotype (see below).

To determine the role of H3R2me2a within euchromatin, we divided 5,065 genes into five groups according to their transcriptional rate[13] (designated by shades of blue in Fig. 2a). We then examined the average enrichment of H3R2me2a for each gene group.

[1]Gurdon Institute and Department of Pathology, Tennis Court Road, Cambridge CB2 1QN, UK. [2]Wellcome Trust Sanger Institute, Hinxton, Cambridge CB10 1HH, UK. [3]NimbleGen Systems, Inc., 1 Science Court, Madison, Wisconsin 53711, USA. [4]Max Planck Institute for Biochemistry, Department of Proteomics and Signal Transduction, D-82152 Martinsried, Germany.

Composite profiles indicate that H3R2me2a occurs near the middle of the coding region and peaks towards the 3′ end of genes (Fig. 2a). The H3R2me2a enrichment is inversely correlated with transcriptional activity because this mark is most abundant on the least active genes.

A role for H3R2 methylation in transcriptional repression was also highlighted by comparing its genomic profile with the pattern of H3K4me3, which is a signal for active transcription. Figure 2b shows that H3K4me3 is found at the 5′ end of genes, which is consistent with previous studies[14,15], and that it is most enriched at the most active genes (darker shades of blue). We noticed that H3K4me3 is enriched in the region of a gene at which H3R2me2a is missing, suggesting an antagonistic relationship between these two modifications (Fig. 2a, b).

To investigate the relationship of H3R2me2a with all H3K4 methyl states we divided all genes into three transcriptional categories (inactive, moderately transcribed and highly transcribed) and then compared the distribution of H3R2me2a with that of the three methyl-H3K4 marks (H3K4me1, H3K4me2 and H3K4me3) across individual genes. In all three transcriptional states the pattern of H3R2me2a was mutually exclusive with H3K4me3 specifically (Fig. 2c–e and Supplementary Fig. 4). This inverse enrichment between H3R2me2a and H3K4me3 is not seen with trimethylation of the other two known modified lysines in yeast, H3K36me3 and H3K79me3 (data not shown). The inverse profiles of H3R2me2a and H3K4me3 were not due to failure of the anti-H3R2me2a and anti-H3K4me3 antibodies to recognize their epitope when the adjacent residue is methylated (Supplementary Fig. 1c). These results indicate that H3R2me2a covers the promoter and coding region of silent genes but, as the transcription rate is increased, H3R2me2a recedes from the 5′ end and is replaced by H3K4 trimethylation.

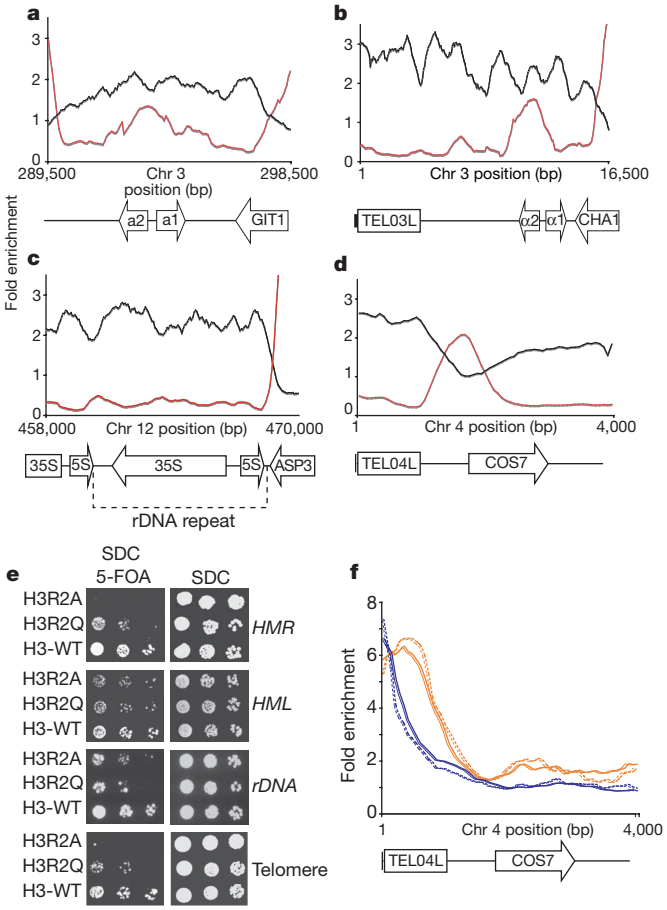

Figure 1 | H3R2me2a associates with heterochromatin. **a**–**d**, ChIP-on-chip analysis was performed in wild-type yeast cells (BY4741) grown to mid-exponential phase with the use of antibodies against H3R2me2a (black lines) and H3K4me3 (red lines). The graphs show a moving average (window = 15, step = 1) of the H3R2me2a and H3K4me3 enrichment normalized to histone H3 occupancy at the right (*HMR*, **a**) and left (*HML*, **b**) mating-type cassettes, at the silent ribosomal DNA repeat region (*rDNA*, **c**) and at the left telomere of chromosome 4 (*TEL04L*, **d**). Values less than 1 indicate regions that are not enriched. The arrows at the bottom of the graphs represent the locations of genes and the direction in which each is transcribed. The rectangles at the bottom of the graphs correspond to the telomeric sequences. bp, base pairs. **e**, Heterochromatin silencing assays were performed on cells from the H3R2A, H3R2Q and isogenic wild-type (H3-WT) yeast strains. Plates were photographed after incubation for 48 h at 30 °C. **f**, ChIP-on-chip analysis on telomeres with the use of antibodies against Sir2p (orange) and Rap1p (blue) in WT (solid lines) and H3R2A (dashed lines) strains. The graph shows a moving average (window = 15, step = 1) of the antibody enrichment over input at *TEL04L*.

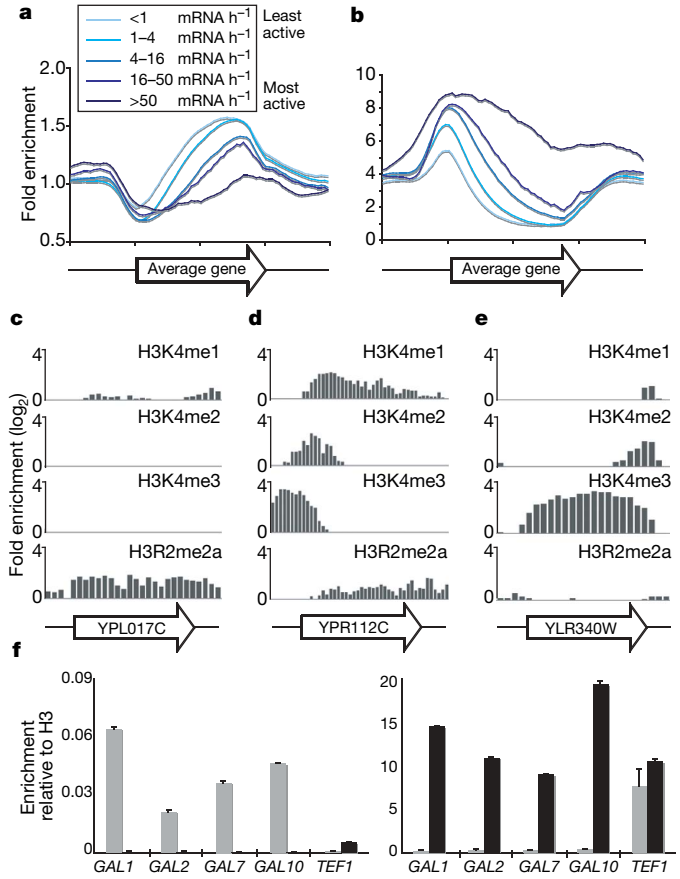

Figure 2 | H3R2me2a enrichment at euchromatic genes is mutually exclusive with H3K4me3. **a**, **b**, ChIP-on-chip analysis was performed in wild-type yeast cells (BY4741) grown to mid-exponential phase with the anti-H3R2me2a and anti-H3K4me3 antibodies. The graphs represent composite profiles of H3R2me2a (**a**) and H3K4me3 (**b**) at 5,065 genes, which were divided into five groups according to their transcriptional rate[12], shown as different shades of blue (defined in **a**). **c**–**e**, ChIP-on-chip analysis was performed as above, with antibodies against H3K4me1, H3K4me2, H3K4me3 and H3R2me2a. The distribution of these modifications is compared at three differentially expressed genes: an inactive gene (**c**), a moderately transcribed gene (**d**) and a highly transcribed gene (**e**). The name of each gene (arrow) is shown at the bottom of the graphs. **f**, ChIP experiments were performed in yeast cells grown in either glucose (repressed condition; grey bars) or galactose as carbon source (active condition; black bars) with antibodies against H3R2me2a (left) and H3K4me3 (right). The precipitated DNA was analysed by quantitative PCR (RT–PCR) with primers specific for the indicated genes. Error bars indicate s.e.m. for duplicate experiments. The induction of gene expression from glucose-containing to galactose-containing medium was monitored by reverse-transcriptase-mediated PCR analysis (see Supplementary Fig. 9).

We next examined whether H3R2me2a and H3K4me3 are dynamically exchanged on nucleosomes when gene expression is induced. ChIP analysis of cells grown in repressive conditions (glucose) showed high enrichment of H3R2me2a at *GAL* genes, whereas H3K4me3 was not detected at all on the same loci (Fig. 2f, grey bars). Shifting the cells to activating conditions (galactose) completely reversed the levels of the two modifications at those same locations (Fig. 2f, black bars). This analysis confirms the inverse correlation observed between H3R2me2a and H3K4me3, and shows that the two modifications are dynamically regulated together in the sense that when one mark is removed from nucleosomes the other is incorporated.

The dynamic exchange of these two modifications on nucleosomes suggested that the arginine residue at position 2 of histone H3 might have a direct function in regulating the methylation at the adjacent lysine 4. We examined this possibility by analysing the global methylation levels at H3K4 in yeast strains carrying mutations at H3R2 (H3R2A, H3R2Q and H3R2K). Figure 3a and Supplementary Fig. 2 show that in the H3R2A and H3R2Q strains the H3K4me3 signal is abolished, whereas in the H3R2K strain the H3K4me3 signal is greatly reduced. The H3K4me1 and H3K4me2 are, respectively, unaffected or very slightly reduced in these mutant strains (Fig. 3a, lane 3, and Supplementary Fig. 2, lanes 2–4). The disruption of H3K4me3 by mutating H3R2 is specific, because the H3R2A mutation does not affect the trimethyl state at the other methylated sites, namely H3K36 and H3K79 (Fig. 3a, lane 3). The loss of the H3K4me3 signal in the H3R2A mutant is not due to failure of the anti-H3K4me3 antibody to recognize its epitope when arginine 2 is mutated (Supplementary Fig. 5, lane 3, left and right panels).

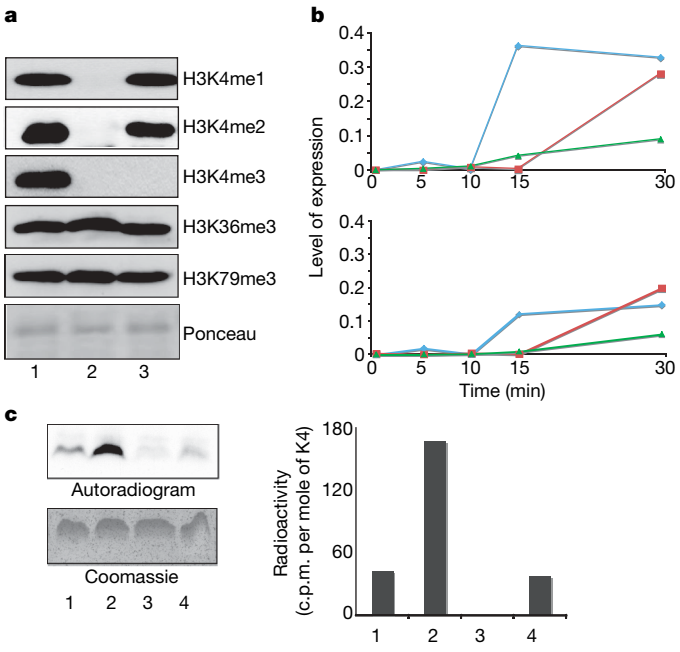

Figure 3 | H3R2me2a regulates the activity of the Set1 complex towards H3K4. a, Whole yeast extracts prepared from the H3R2A (lane 3), *set1C1068A* (lane 2) and isogenic WT (lane 1) strains were analysed by western blotting with antibodies against H3K4me1, H3K4me2, H3K4me3, H3K36me3 or H3K79me3. Uniform loading was monitored by Ponceau stain. **b**, Yeast cells expressing WT (blue), R2A mutant (red) or K4A mutant (green) histone H3 were grown to mid-exponential phase in medium containing raffinose (inactive condition) and then shifted to medium containing galactose (activating condition). RNA was prepared at the indicated times and analysed by quantitative RT–PCR with primers specific for *GAL7* (top) and *GAL1* (bottom). Values show the expression of *GAL7* or *GAL1* normalized to the RNA levels of *RTG2*, whose expression remains unchanged. The experiment was repeated with similar results. **c**, Purified Set1 complex from yeast was incubated with *S*-[^{3}H]adenosylmethionine in the presence of H3R2me2a (residues 1–17, lane 1), an unmodified peptide (residues 1–17, lane 2), H3K4me3 (residues 1–17, lane 3) or H3R2A mutant (residues 1–17, lane 4). Peptides were analysed for radioactive labelling with the use of autoradiography (activity on peptides; left) or sequential Edman degradation (activity on lysine 4; right). Equal loading of peptides was monitored by Coomassie stain (bottom left). The radioactivity released at lysine 4 of the H3K4me3 peptide (lane 3) was regarded as background signal and was subtracted from the lysine 4 signals of the other three peptides (right). The methylase assay was repeated three times with similar results.

The fact that trimethylation of H3K4 defines active transcription[16] prompted us to examine whether the H3R2A mutation affected gene expression. We tested the kinetics of *GAL1* and *GAL7* induction in the wild type and in H3R2A and H3K4A mutant strains. Figure 3b shows that mutation of H3R2 delays the activation of *GAL* genes. The effect of the H3R2A mutation is similar to, but less severe than, that of the H3K4A mutation, indicating that these two residues might be involved in a common regulatory mechanism (Fig. 3b).

We next sought to determine the mechanism responsible for the inverse distribution between H3R2me2 and H3K4me3. We first considered the possibility that H3R2 forms part of the recognition site for the Set1 complex, which methylates H3K4. Figure 3c shows that purified Set1 complex from yeast is able to methylate an unmodified H3 peptide but its activity is inhibited by mutation of arginine 2 to alanine (compare lane 2 with lane 4). Asymmetric dimethylation at H3R2 also inhibits the activity of the Set1 complex towards lysine 4 (Fig. 3c, compare lane 1 with lane 2). This Set1p activity is specific for lysine 4, because a peptide that is already trimethylated at H3K4 shows only background signal (Fig. 3c, lane 3). In addition, peptide sequencing reveals that the activity of the Set1 complex is occurring only at residue 4 (Supplementary Fig. 6). These results indicate that H3R2 is a recognition site for the Set1p methylase complex and also that methylation of H3R2 inhibits the Set1p enzyme from methylating H3K4.

The ability of Set1p to catalyse monomethylation, dimethylation or trimethylation at H3K4 is regulated by several components of the Set1 complex. Specifically, the Spp1 subunit is required for Set1-mediated trimethylation of H3K4 (ref. 10). It has been shown recently that Spp1 binds specifically to H3K4me2 and H3K4me3 through its PHD domain[17]. We therefore examined whether methylation of H3R2 is required for the binding of Spp1 to methylated lysine 4 *in vitro*. Figure 4a shows that dimethylation of H3R2 inhibits the interaction of the Spp1 PHD finger with dimethylated or trimethylated K4 (compare lanes 3 and 5 with lanes 4 and 6). Mutation of H3R2 also disrupts the binding of Spp1, which is consistent with the fact that this arginine residue is part of the recognition site of the Spp1 PHD finger[17] (Supplementary Fig. 7). To determine whether H3R2me2a also blocks Spp1 binding *in vivo* we performed ChIP assays in a yeast strain expressing Myc-tagged Spp1. Figure 4b and Supplementary Fig. 8 show that Spp1 is bound to regions of genes that were trimethylated at H3K4 and were devoid of H3R2me2a. However, Spp1 was absent from areas of genes at which H3R2 methylation was present, even though H3K4me1 or H3K4me2 was also abundant in these regions (Fig. 4b, middle panel, and Supplementary Fig. 8). These results confirm the biochemical analysis in Fig. 4a, which shows that H3R2 methylation can prevent Spp1 from binding H3K4me2. Moreover, the above observations that H3K4me3 is absent from regions in which H3R2me2a is enriched are consistent with the occlusion of Spp1.

Together these results identify the existence and indicate the function of H3R2 methylation in yeast. H3R2 methylation regulates the activity of the Set1 complex towards H3K4 by modulating the binding of its Spp1 component. The role of H3R2me2a in controlling H3K4me3 is also conserved in humans[18], indicating that this mechanism is likely to be generally applicable in all eukaryotes.

These findings place methylation at H3R2 and H3K4 in the same pathway and support a role of H3R2me2a as a negative regulator of H3K4 trimethylation. Figure 4c shows a model of how H3R2me2a may function during the transition from a repressed to a transcriptionally active state on a gene. Global analysis shows that when a gene

is inactive, H3R2me2a is present throughout the promoter and coding region (step 0). Methylation of H3R2 in yeast is likely to be catalysed by a previously unknown and as yet unidentified methyltransferase, because combinatorial deletion of the three known arginine methyltransferases (Rmt1, Rmt2 and Hsl7) does not affect the degree of this modification (data not shown). At this silent stage (step 0) very little, if any, methylation of H3K4 takes place. During activation, the presence of methylated H3R2 does not inhibit Set1p from monomethylating or dimethylating H3K4 (step 1). However, for trimethylation of H3K4 to take place, methylation at H3R2 has to be removed (step 2). The clearing of methylation at H3R2 must be mediated either by histone replacement or by the action of an as yet unidentified arginine demethylase. Once a region becomes devoid of H3R2 methylation, the Spp1 protein can recognize H3K4me2 by its PHD domain. This binding probably extends the time of interaction between the Set1 complex and its substrate, thus promoting the trimethylation of H3K4 by Set1p (step 3 (ref. 19)). Spp1 then associates with H3K4me3 (step 4), possibly to protect this methyl state from the action of the H3K4me3 demethylase Jhd2 (refs 20, 21). At the same time, Spp1 may protect H3R2 from methylation; structural studies[17,22,23] have shown that this arginine residue is absolutely required for the association of the Spp1 PHD finger with methylated H3K4. Together these data indicate that arginine methylation at H3R2 may influence transcription by regulating the H3K4 trimethylation capacity of the Set1 methyltransferase.

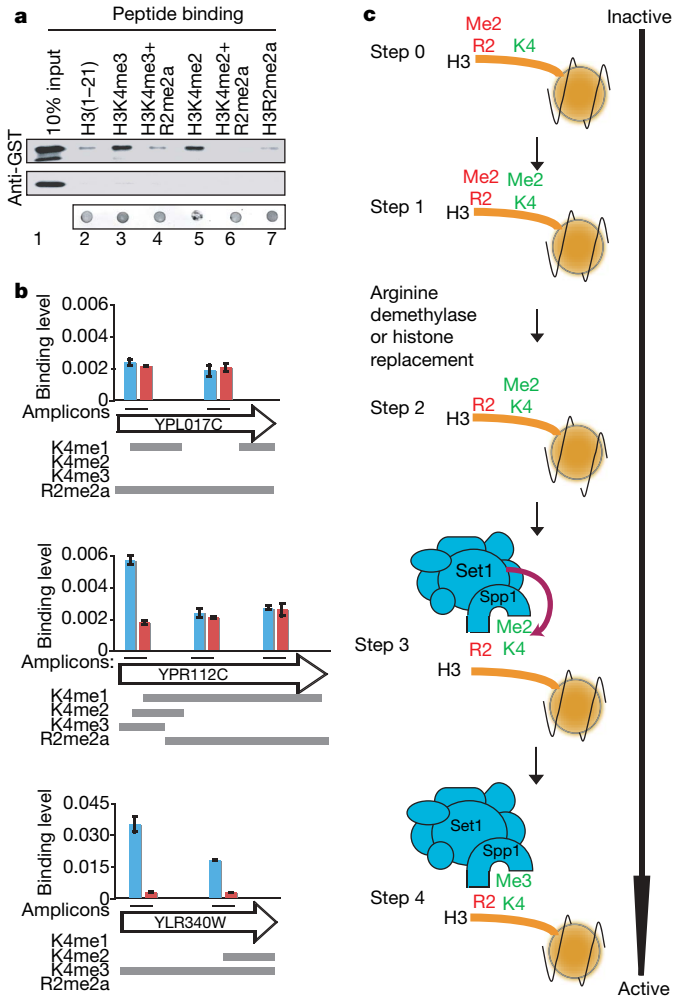

Figure 4 | H3R2me2a blocks the binding of Spp1 to methylated H3K4. **a**, *In vitro* binding assays were performed with synthetic N-terminal peptides (residues 1–21) of histone H3 and either recombinant glutathione *S*-transferase (GST)-conjugated $Spp1_{PHD}$ (top) or GST alone (middle). The bound proteins were monitored by western blot analysis with an anti-GST antibody. Peptide coupling was controlled by dot-blotting followed by Coomassie staining (bottom). **b**, *In vivo* binding analysis of Spp1 was performed with ChIP assays followed by quantitative PCR. Chromatin from yeast cells expressing a Myc-tagged (blue columns) or an untagged (red columns) form of Spp1 was immunoprecipitated with anti-Myc antibody. Three differentially expressed genes were examined: an inactive gene (top), a moderately transcribed gene (middle) and a highly transcribed gene (bottom). The analysed amplicons within each gene (named within the arrow) are indicated by black lines. Error bars indicate s.e.m. for duplicate experiments. The grey bars below each plot show the distribution of H3K4me1, H3K4me2, H3K4me3 and H3R2me2a within each gene. **c**, Model of how methylation at histone H3R2 controls trimethylation at H3K4.

METHODS SUMMARY

Formaldehyde crosslinking and ChIP were performed as described previously[24], with the following exceptions: the immunocomplexes were eluted from the Sepharose beads (17-5280-01; Amersham) using a total of 200 µl of elution buffer (100 mM sodium bicarbonate, 1% SDS), and treatment with RNase (11119915001; Roche) was performed during reversal of the crosslinks at 65 °C for 5 h. After reversal of the crosslinks, each individual ChIP sample was purified with the Qiaquick polymerase chain reaction (PCR) purification kit (Qiagen) and DNA was eluted from the columns with 50 µl of EB buffer (10 mM Tris-HCl pH 8.5). Amplicons were generated from individual ChIP samples by using a linker-mediated PCR. Sample labelling, hybridization and data extraction were performed by NimbleGen Systems Inc. as part of a ChIP Array Service. Downstream analysis of the ChIP-on-chip data was performed with the statistical package R (www.R-project.org) and associated array analysis modules in Bioconductor.

Full Methods and any associated references are available in the online version of the paper at www.nature.com/nature.

Received 15 March; accepted 9 August 2007.
Published online 26 September 2007.

1. Kouzarides, T. Chromatin modifications and their function. *Cell* **128,** 693–705 (2007).
2. Martin, C. & Zhang, Y. The diverse functions of histone lysine methylation. *Nature Rev. Mol. Cell Biol.* **6,** 838–849 (2005).
3. Wysocka, J., Allis, C. D. & Coonrod, S. Histone arginine methylation and its dynamic regulation. *Front. Biosci.* **11,** 344–355 (2006).
4. Ruthenburg, A. J., Allis, C. D. & Wysocka, J. Methylation of lysine 4 on histone H3: intricacy of writing and reading a single epigenetic mark. *Mol. Cell* **25,** 15–30 (2007).
5. Sims, R. J. & Reinberg, D. Histone H3 Lys 4 methylation: caught in a bind? *Genes Dev.* **20,** 2779–2786 (2006).
6. Torres-Padilla, M. E., Parfitt, D. E., Kouzarides, T. & Zernicka-Goetz, M. Histone arginine methylation regulates pluripotency in the early mouse embryo. *Nature* **445,** 214–218 (2007).
7. Shi, X. *et al.* ING2 PHD domain links histone H3 lysine 4 methylation to active gene repression. *Nature* **442,** 96–99 (2006).
8. Wysocka, J. *et al.* A PHD finger of NURF couples histone H3 lysine 4 trimethylation with chromatin remodelling. *Nature* **442,** 86–90 (2006).
9. Dou, Y. *et al.* Regulation of MLL1 H3K4 methyltransferase activity by its core components. *Nature Struct. Mol. Biol.* **13,** 713–719 (2006).
10. Schneider, J. *et al.* Molecular regulation of histone H3 trimethylation by COMPASS and the regulation of gene expression. *Mol. Cell* **19,** 849–856 (2005).
11. Steward, M. M. *et al.* Molecular regulation of H3K4 trimethylation by ASH2L, a shared subunit of MLL complexes. *Nature Struct. Mol. Biol.* **13,** 852–854 (2006).
12. Schurter, B. T. *et al.* Methylation of histone H3 by coactivator-associated arginine methyltransferase 1. *Biochemistry* **40,** 5747–5756 (2001).
13. Holstege, F. C. *et al.* Dissecting the regulatory circuitry of a eukaryotic genome. *Cell* **95,** 717–728 (1998).
14. Liu, C. L. *et al.* Single-nucleosome mapping of histone modifications in *S. cerevisiae*. *PLoS Biol.* **3,** e328 (2005).
15. Pokholok, D. K. *et al.* Genome-wide map of nucleosome acetylation and methylation in yeast. *Cell* **122,** 517–527 (2005).
16. Santos-Rosa, H. *et al.* Active genes are tri-methylated at K4 of histone H3. *Nature* **419,** 407–411 (2002).
17. Shi, X. *et al.* Proteome-wide analysis in *Saccharomyces cerevisiae* identifies several PHD fingers as novel direct and selective binding modules of histone H3 methylated at either lysine 4 or lysine 36. *J. Biol. Chem.* **282,** 2450–2455 (2007).
18. Guccione, E. *et al.* Methylation of histone H3R2 by PRMT6 and H3K4 by an MLL complex are mutually exclusive. *Nature* doi:10.1038/nature06166 (this issue).
19. Wood, A. *et al.* Ctk complex-mediated regulation of histone methylation by COMPASS. *Mol. Cell. Biol.* **27,** 709–720 (2007).
20. Liang, G., Klose, R. J., Gardner, K. E. & Zhang, Y. Yeast Jhd2p is a histone H3 Lys4 trimethyl demethylase. *Nature Struct. Mol. Biol.* **14,** 243–245 (2007).

21. Seward, D. J. *et al.* Demethylation of trimethylated histone H3 Lys4 *in vivo* by JARID1 JmjC proteins. *Nature Struct. Mol. Biol.* **14,** 240–242 (2007).
22. Li, H. *et al.* Molecular basis for site-specific read-out of histone H3K4me3 by the BPTF PHD finger of NURF. *Nature* **442,** 91–95 (2006).
23. Pena, P. V. *et al.* Molecular mechanism of histone H3K4me3 recognition by plant homeodomain of ING2. *Nature* **442,** 100–103 (2006).
24. Morillon, A., O'Sullivan, J., Azad, A., Proudfoot, N. & Mellor, J. Regulation of elongating RNA polymerase II by forkhead transcription factors in yeast. *Science* **300,** 492–495 (2003).

Supplementary Information is linked to the online version of the paper at www.nature.com/nature.

Acknowledgements We thank C. Nelson, A. Bannister and M. Christophorou for critical reading of the manuscript; S. Marguerat for helpful discussions; L. Packman and M. Weldon for assistance with protein sequencing; N. Jiang and R. Selzer for assistance with microarray analyses; and M. Gilchrist for help with displaying genomic data. This work was supported by postdoctoral fellowship grants to A.K. from the European Molecular Biology Organization (EMBO) and Marie Curie. The T.K. laboratory is funded by grants from Cancer Research UK (CRUK) and the 6th Research Framework Programme of the European Union (Epitron and Heroic).

Author Information The microarray data sets are available from GEO (Gene Expression Omnibus) under accession number GSE8626, and from http://www.gurdon.cam.ac.uk/%7Ekouzarideslab/H3R2methylation.html. Reprints and permissions information is available at www.nature.com/reprints. The authors declare competing financial interests: details accompany the full-text HTML version of the paper on www.nature.com/nature. Correspondence and requests for materials should be addressed to T.K. (t.kouzarides@gurdon.cam.ac.uk).

METHODS

Yeast strains and plasmids. The following *Saccharomyces cerevisiae* strains were used: wild-type (BY4741; Open Biosystems): *MAT***a**, *ura3-0*, *leu2Δ0*, *his3Δ1*, *met15Δ0*; JHY6: *MAT***a**, *ura3-52*, *lys2-801*, *ade2-101*, *trp*1−289, *his3Δ1*, *leu2*−3,112, Δ*hhf2-hht2*, Δ*hhf1-hht1*, pMS333[URA3-*HHT2-HHF2*]; UCC1369: *MAT***a**, *ade2::hisG*, *his3Δ200*, *leu2Δ0*, *lys2Δ0*, *met15Δ0*, *trp1Δ63*, *ura3Δ0*, *adh4::URA3-TEL-VIIL*, *ADE2-TEL-VR*, *hhf2-hht2::MET15*, *hhf1-hht1::LEU2*, pMP9; UCC1188: *MATα*, *leu2Δ1*, *lys2-801*, *trp1*, *ura3*, *RDN1::URA3*, *hhf2-hht2::HIS3*, *hhf1-hht1::LEU2*, pMP9; UCC7262: *MAT***a**, *ade2*, *his3*, *leu2*, *lys2*, *ura3*, *ADE2-TEL-VR*, *hhf2-hht2::MET15*, *hhf1-hht1::LEU2*, *hmra::URA3*, pMP9; UCC7266: *MAT***a**, *ade2*, *his3*, *leu2*, *lys2*, *ura3*, *ADE2-TEL-VR*, *hhf2-hht2::MET15*, *hhf1-hht1::LEU2*, *hml::URA3*, pMP9. C13 ABYS-86: *Matα ura3 leu2-3 his3-112 pra1-1 prb1-1 prc1-1 cps1-3*. Mutations of H3R2 and H3K4 were introduced into the *HHT2* gene in plasmid pMR206 (*TRP1-HHT2-HHF2*) using the QuickChange site-directed mutagenesis kit (Stratagene) and verified by sequencing. Mutant and wild-type control plasmids were introduced into strain JHY6 to make the strains JHY6-H3WT, JHY6-H3R2A, JHY6-H3R2Q and JHY6H3K4A. Derivatives of pMR206 were also used to replace plasmid pMP9 in strains UCC1369, UCC1188, UCC7262 and UCC7266 to make the following strains: UCC1369-H3WT, UCC1369-H3R2A, UCC1369-H3R2Q, UCC1188-H3WT, UCC1188-H3R2A, UCC1188-H3R2Q, UCC7262-H3WT, UCC7262-H3R2A, UCC7262-H3R2Q, UCC7266-H3WT, UCC7266-H3R2A and UCC7266-H3R2Q. Strain JHY6-H3WT was also used in PCR-mediated disruption to create strains JHY6-*set1C1068A* (*set1C1068A::HIS3*) and JHY6-*Sir2Δ* (*sir2::KAN*). Strain JHY6 was a gift from S. Berger, strain C13 ABYS-86 was a gift from D. H. Wolf, and strains UCC1369, UCC1188, UCC7262 and UCC7266 were gifts from D. Gottschling.

Western blotting. Yeast cells were grown to mid-exponential phase in rich medium in a 30 °C shaker. Total yeast extracts were prepared by first resuspending cell pellets in a tenfold volume of SDS loading buffer (3% 2-mercaptoethanol, 3% SDS, 0.1% bromophenol blue, 10% glycerol) and then the samples were alternately boiled and chilled three times to rupture cell membranes. Core calf thymus histones were obtained from Roche Applied Sciences. Acid extraction was used to prepare histones from H3K293 and C3H10T1/2 cells, which were cultured in DMEM medium supplemented with 10% FBS in a 5% CO_2 incubator at 37 °C. Western blotting was performed with standard procedures. The nitrocellulose membranes (Whatman) were blocked overnight in BSA buffer (Tris-buffered saline, 0.01% Tween 20, 5% BSA) at 4 °C. The antibodies used included anti-H3 (ab1791; Abcam), anti-H3R2me2a (ab8046; Abcam), anti-H3K4me1 (ab8895; Abcam), anti-H3K4me2 (ab7766; Abcam), anti-H3K4me3 (ab8580; Abcam), anti-H3K36me3 (ab9050; Abcam) and anti-H3K79me3 (ab2621; Abcam).

Antibody characterization. Dot-blotting was performed as described previously[25]. In brief, 2 μl of peptide dilutions were spotted on poly(vinylidene difluoride) (PVDF) membranes (RPN2020F; Amersham) and left to air-dry. The membranes were then blocked for 2 h with BSA buffer (Tris-buffered saline, 0.01% Tween 20 and 5% BSA) at room temperature (22–25 °C) before a standard immunoblot analysis was performed. For peptide competitions, 500 ng of isolated yeast histones, prepared as described below, were separated by 15% SDS–PAGE. A standard western blotting procedure was followed except that the antibodies were incubated with the peptides (0.5 μg ml^{-1}) for 30 min at room temperature before the membranes were probed. The antibodies used included anti-H3, anti-H3R2me2a and anti-H3K4me3.

The specificity of the anti-H3R2me2a antibody is further validated by the fact that its reactivity towards mammalian histones is sensitive to the deletion of CARM1/PRMT4 (ref. 6). This shows that the antibody is specific for methylated H3R2 because deletion of the enzyme (CARM1) that catalyses this modification *in vitro*[12] affects the antibody.

Yeast histone/chromatin preparation. Cells were grown to mid-exponential phase in rich medium (YPD), washed once in PBS and resuspended in Spheroplasting buffer (0.6 M sorbitol, 20 mM potassium phosphate pH 7.0, 5 mg of zymolase 20T per g of cells). After incubation for 30 min at room temperature with gentle shaking, cells were centrifuged at 3,500 r.p.m. for 10 min and washed once with 0.6 M sorbitol in 20 mM potassium phosphate pH 7.0). The cell pellet was then resuspended in 4 ml of Ficoll buffer (18% Ficoll, 20 mM PIPES pH 6.3, 0.5 mM $CaCl_2$, 1 mM dithiothreitol (DTT), 1 mM EDTA) per g of cells, disrupted by five or six strokes in a manual Dounce homogenizer and centrifuged at 6,000 r.p.m. for 10 min. The supernatant was discarded. Pelleted cells were resuspended in 10 ml of extraction buffer (10 mM HEPES pH 7.5, 1 mM EDTA, 0.5 M NaCl, 0.5% Nonidet P40), incubated on ice for 20 min and centrifuged at 14,000 r.p.m. for 10 min. The supernatant was discarded. The washes with extraction buffer were repeated until the pellet started to lose opacity. The pellet was then resuspended in 2 ml of Tris-HCl pH 8, 10% glycerol and dialysed overnight against the same buffer. Finally the sample was divided into aliquots and stored at −80 °C.

Chromatin immunoprecipitation. Wild-type (BY4741), JHY6-H3WT and JHY6-H3R2A strains were grown to mid-exponential phase in a 30 °C shaker. For the galactose induction experiments BY4741 cells were cultured overnight in complete medium (YPD) containing 2% glucose. The next morning the cells were split into two YPD samples, one containing 2% glucose and the other 2% galactose, and grown at 30 °C for a further 24 h. Cell pellets from both conditions collected at mid-exponential phase were used for ChIP experiments and RT–PCR (see below). The following antibodies were used for immunoprecipitation: 3 μl of anti-H3 per immunoprecipitation (IP), 3 μl/IP of anti-H3K4me3, 3 μl/IP of anti-H3K4me2, 3 μl per IP of anti-H3K4me1, 3 μl per IP of anti-H3R2me2a, 25 μl per IP of anti-Rap1 (sc-6663; Santa Cruz Biotechnology), 25 μl per IP of anti-Sir2 (sc-6667; Santa Cruz Biotechnology) and, as a negative control, 2 μl per IP of rabbit anti-mouse IgG (5180-2104; Biogenesis).

ChIP-on-chip data analysis. Primer positions were mapped with exonerate[26], and this information, along with an *S. cerevisiae* gff annotation file, was read into an R data structure with the use of scripts from the Bioconductor package tilingArray[27]. Raw NimbleGen output files were used for the analysis of the data. Two channels were used for each array; for each channel, the biweight mean for all data points was calculated and used to scale the data. The corrected data were then used to calculate a ratio of immunoprecipitated to control DNA for each spot. Finally, a ratio of these data to similarly corrected histone H3 data was used to normalize the data to nucleosome occupancy levels. Composite average profiles were created in a similar manner to that described previously[15]. The ends of open reading frames (ORFs) were defined at fixed points corresponding to the positions of translational start and stop sites. The length of the ORF was then subdivided into 40 regions of equal length, and the middle of each probe was assigned according to its nearest relative bin position. Probes 800 base pairs (bp) before start sites and 800 bp after stop sites were similarly assigned after subdivision into 20 bins for both regions.

Real-time PCR. Real-time PCR analysis was performed on an ABI PRISM 7000 sequence detection system with the use of SYBR Green (Applied Biosystems) as described previously[28]. In brief, standard curves for each primer set were calculated from amplification of wild-type genomic DNA diluted 1:10, 1:100. 1:1,000, 1:10,000 and 1:100,000. After each run, a dissociation curve was performed to ensure that no primer dimers contaminated the quantification and that the product had the expected melting temperature. Each PCR reaction was performed in duplicate and the analysis was repeated twice from independent ChIP experiments. A signal intensity value for each sample was calculated from the average of the two experiments. Relative fluorescent intensities for the ChIP experiments were calculated as follows: $[(\text{Ab signal}_X/\text{Ab signal}_Y) - (\text{IgG signal}_X/\text{IgG signal}_Y)]/[(\text{H3 signal}_X/\text{H3 signal}_Y) - (\text{IgG signal}_X/\text{IgG signal}_Y)]$, where Ab is the antibody of interest, IgG is the negative control antibody, H3 is the histone H3 antibody, X is the locus of interest and Y is the intergenic region on chromosome V that was used as an internal background control. The sequences of the primers used for PCR analysis are shown in Supplementary Table 1.

Quantitative RT–PCR. Total yeast RNA was prepared from 3×10^7 cells of each indicated growth condition using the RNeasy Mini kit (Qiagen) in accordance with the manufacturer's protocol. To ensure complete removal of contaminating DNA from the RNA preparations, the Turbo DNA-free kit (Ambion) was used. First-strand complementary DNA synthesis was achieved with SuperScript II reverse transcriptase (catalogue no. 18080; Invitrogen) with a primer cocktail containing 50 μM oligo(dT) (Ambion) and 50 ng of random hexamers (Invitrogen), as described in the manufacturer's instructions. The cDNA samples were then used as templates for real-time PCR (see above).

Array design. The *S. cerevisiae* genome tiling array contained a total of 379,521 50-mer oligonucleotides, positioned every 64 bp throughout the yeast genome representing both DNA strands. The design included random GC probes as controls.

Peptide synthesis. Peptides corresponding to amino-acid residues 1–17 of histone H3 were synthesized in house using the Fmoc strategy on a solid-phase peptide synthesizer (Intavis). Peptides were synthesized on amide resin as 20-mers containing the first 17 amino acids of the amino-terminal tail of histone H3 followed by a double glycine spacer and a biotinylated lysine residue on the carboxy terminus. Unmodified amino acids as well as methylated arginine and lysine derivatives used for the synthesis were purchased from Novagen or Bachem. After synthesis, peptides were cleaved from the resin with trifluoroacetic acid, precipitated with ether, and dried in air. The identity and quality of the peptides were checked by mass spectrometry. Histone H3 N-terminal peptides corresponding to residues 1–8 and 1–21 were obtained from Almac Sciences. Peptides were synthesized with at least 90% purity and were resuspended in 10 mM HEPES pH 7.5 containing 0.005% Igepal (Sigma).

***In vitro* methyltransferase and peptide pull-down assays.** Purification of the Set1 complex and the methyltransferase assay were performed as described[16]. Protein-A–Set1 was expressed and the Set1 complex was purified from the C13 ABYS-86 strain. About 1 μg of Set1 complex was incubated in 50 mM Tris-HCl pH 8.5, 20 mM KCl, 10 mM $MgCl_2$, 10 mM 2-mercaptoethanol, 0.05 mM DTT, 250 mM sucrose, 0.2% dodecyl-β-D-maltoside buffer, with 2 μl of *S*-adenosyl-L-[Me-^{3}H]methionine (TRK865; Amersham Pharmacia) and about 2 μg of peptides corresponding to residues 1–17 of histone H3 as substrate, for 1 h at 30 °C. The reactions were resolved in 17% Tricine gels, transferred by Western blotting to PVDF membrane and exposed to KodaK Biomax MS autoradiogram films for 12 h. Peptides in the reaction were also revealed by Coomassie staining of the PVDF membrane, cut off and subjected to Edman degradation at the PNAC facility, University of Cambridge (www.bioc.cam.ac.uk/pnac/proteinsequencing.html) followed by quantification in a scintillation counter (LS6500; Beckman Coulter). The molar concentration of each peptide was determined from the amount of the first alanine residue present in each peptide. The radioactive counts released from each peptide were then normalized to the molar concentration of each peptide.

The Spp1 PHD domain, covering amino acids 20–76, was amplified from genomic yeast DNA and cloned into vector pGEX-5X-1. Binding assays with 3 μg of GST–$Spp1_{PHD}$ and 20 μg of N-terminal H3 peptides were performed as described previously[29], with minor modifications. The binding was performed overnight at 4 °C in PDB-150 buffer (50 mM Tris-HCl pH 8.0, 150 mM NaCl, 10 μM $ZnCl_2$, 5 mM EDTA, 0.5% Igepal, containing protease inhibitor cocktail (Roche Applied Sciences)), followed by washing in PDB-150.

25. Perez-Burgos, L. *et al.* Generation and characterization of methyl-lysine histone antibodies. *Methods Enzymol.* **376,** 234–254 (2004).
26. Slater, G. S. & Birney, E. Automated generation of heuristics for biological sequence comparison. *BMC Bioinformatics* **6,** 31 (2005).
27. David, L. *et al.* A high-resolution map of transcription in the yeast genome. *Proc. Natl Acad. Sci. USA* **103,** 5320–5325 (2006).
28. Santos-Rosa, H. *et al.* Methylation of histone H3 K4 mediates association of the Isw1p ATPase with chromatin. *Mol. Cell* **12,** 1325–1332 (2003).
29. Nelson, C. J., Santos-Rosa, H. & Kouzarides, T. Proline isomerization of histone H3 regulates lysine methylation and gene expression. *Cell* **126,** 905–916 (2006).